Technobius Physics, 2026, 4(2), 0052, DOI: https://doi.org/10.54355/tbusphys/30070147.4.2.2026.0052

Technobius Physics

https://technobiusphysics.kz/

e-ISSN 3007-0147

Article

Physics-Informed Neural Networks for modeling heat diffusion in anisotropic solids

Saira Sakhabayeva*

Department of Physics, Nazarbayev University, Astana, Kazakhstan
*Correspondence: saira.sakhabayeva@nu.edu.kz

Abstract. Accurate simulation of heat diffusion in anisotropic solids is essential for the design and optimization of advanced engineering materials and thermal management systems. However, conventional numerical approaches often require computationally intensive mesh generation and repeated solution procedures, particularly for transient problems involving directional heat transport. This study investigates the application of Physics-Informed Neural Networks for modeling transient heat diffusion in anisotropic solid materials. The proposed framework incorporates the governing heat conduction equation, initial conditions, and boundary conditions directly into the neural network training process, enabling physically consistent predictions without extensive labeled datasets. The model was trained using a combination of Adam and L-BFGS optimization algorithms and validated against finite element method simulations. The influence of thermal anisotropy was evaluated for conductivity ratios ranging from isotropic conditions to strongly anisotropic cases. The developed Physics-Informed Neural Networks demonstrated excellent agreement with finite element method solutions, achieving a root mean square error of 0.014 K, a mean absolute error of 0.010 K, a maximum absolute error of 0.061 K, and a coefficient of determination of 0.9997. Although prediction errors increased slightly with increasing anisotropy, the model maintained high accuracy and stable convergence across all investigated scenarios. The results confirm that Physics-Informed Neural Networks provide an accurate and physically consistent alternative to traditional numerical methods for anisotropic heat transfer analysis. The proposed approach offers significant potential for rapid thermal simulations, inverse heat transfer problems, digital twin development, and real-time engineering applications involving complex anisotropic materials.

Keywords: Physics-Informed Neural Networks; Heat Diffusion; Anisotropic Solids; Heat Transfer; Scientific Machine Learning; Finite Element Method; Thermal Conductivity Tensor; Computational Physics.

1. Introduction

Heat transfer is one of the most fundamental physical processes governing the behavior of natural and engineered systems. The transport of thermal energy influences the performance, efficiency, reliability, and safety of technologies ranging from microelectronic devices and energy conversion systems to aerospace structures, advanced manufacturing processes, and thermal management systems [1], [2]. Accurate prediction of temperature distributions within solid materials is therefore essential for engineering design, process optimization, and operational control. Among the various heat-transfer mechanisms, thermal conduction plays a dominant role in solids and is commonly described by Fourier's law, which relates heat flux to temperature gradients [3]. The resulting heat diffusion equation provides the theoretical foundation for modeling transient and steady-state thermal processes in a wide range of materials and engineering applications.

In practical engineering systems, however, heat transfer rarely occurs in perfectly isotropic media. Many advanced materials exhibit anisotropic thermal properties, meaning that thermal conductivity varies with direction. Such behavior is characteristic of fiber-reinforced composites, layered structures, crystalline solids, thermoelectric materials, geological formations, thermal barrier

coatings, and emerging multifunctional materials. In anisotropic solids, heat propagates preferentially along specific directions, producing complex temperature fields that are significantly more difficult to predict than those observed in isotropic media [4]. As the use of anisotropic materials continues to expand across engineering and materials science, the development of reliable computational methods capable of accurately modeling directional heat transport has become increasingly important.

The importance of understanding heat-transfer mechanisms extends beyond numerical simulation and remains central to both fundamental and applied physics. Authors [5] investigated heat pump technologies and energy-efficient heating systems, demonstrating that optimized thermal energy management can substantially improve energy utilization and system performance. Their findings emphasize the practical significance of accurately predicting heat-transfer processes in engineering applications. Similarly, authors [6] examined the mechanical equivalent of heat, highlighting the fundamental physical relationship between mechanical work and thermal energy. Their study reinforces the importance of thermal transport phenomena as a cornerstone of modern thermodynamics and energy science. At the materials level, authors [7] investigated potassium-doped copper sulfide compounds and reported transport characteristics relevant to thermoelectric energy conversion. Their work illustrates how thermal transport behavior is strongly influenced by the structural and electronic properties of materials, further motivating the need for advanced predictive models capable of describing heat conduction in complex solids.

Traditionally, heat conduction problems have been solved using numerical approaches such as the finite difference method (FDM), finite volume method (FVM), and finite element method (FEM) [8]. These methods are widely accepted due to their robustness, mathematical rigor, and ability to provide highly accurate solutions. Nevertheless, their application often requires detailed mesh generation, discretization of the computational domain, and significant computational resources, particularly for transient three-dimensional problems involving heterogeneous or anisotropic materials [9]. The computational cost becomes even more significant in optimization studies, uncertainty quantification, inverse heat-transfer problems, and digital-twin applications, where large numbers of simulations may be required.

Recent advances in artificial intelligence and scientific machine learning have created new opportunities for solving physical problems governed by partial differential equations [10], [11]. Deep neural networks have demonstrated exceptional capabilities in approximating nonlinear relationships and high-dimensional functions. However, conventional data-driven neural networks often require large labeled datasets and may produce physically inconsistent solutions when extrapolating beyond the training domain. These limitations have motivated the development of physics-guided machine-learning frameworks that integrate established physical laws directly into the learning process.

One of the most influential developments in this area is the emergence of Physics-Informed Neural Networks (PINNs) [12]. Rather than relying exclusively on observational data, PINNs incorporate governing differential equations, boundary conditions, and initial conditions into the optimization procedure. This approach enables neural networks to learn physically meaningful solutions while reducing dependence on extensive datasets. As a result, PINNs have rapidly become one of the most actively investigated methodologies within scientific machine learning and computational physics [13].

The growing interest in PINNs has resulted in numerous studies focused on diffusion and heat-transfer problems. Authors [14] demonstrated the applicability of PINNs for solving heat equations with source terms under various boundary conditions and reported substantial improvements in physical consistency compared with purely data-driven models. Researchers [15] proposed a mixed-data sampling strategy for diffusion equations and showed that optimized collocation-point selection significantly improves convergence and predictive accuracy. These studies confirmed the ability of PINNs to solve thermal diffusion problems while requiring considerably less training data than conventional machine-learning approaches.

The application of PINNs has subsequently expanded toward increasingly complex thermal systems. Authors [16] employed physics-informed learning to solve the time-dependent mode-

resolved phonon Boltzmann transport equation and demonstrated accurate representation of microscale heat-transfer phenomena. Their work is particularly important because it extends PINN methodologies beyond classical Fourier heat conduction and into regimes where microscopic energy carriers influence thermal transport. Similarly, [17] developed a thermal physics-informed neural network for solving two-dimensional non-Fourier heat conduction equations and reported excellent agreement with reference numerical solutions. These findings indicate that PINNs are capable of describing not only classical diffusion processes but also advanced heat-transfer mechanisms characterized by thermal-wave effects and finite propagation speeds.

Another important area of development concerns the training and optimization of physics-informed models. Scientists [18] demonstrated that affine transformations can significantly accelerate the training process for diffusion-type equations, thereby improving computational efficiency. Researchers [19] applied PINNs to thermally driven cavity-flow simulations and achieved strong agreement with conventional computational fluid dynamics solutions. Authors [20] introduced adaptive fractional PINNs for anomalous heat conduction in functionally graded materials and reported enhanced predictive capability for systems exhibiting non-classical diffusion behavior. These investigations highlight the versatility of PINNs and their growing applicability to increasingly complex thermal systems.

Particularly relevant to the present study are recent investigations involving anisotropic transport phenomena. [21] developed a PINN framework for three-dimensional anisotropic steady-state heat conduction and demonstrated accurate prediction of temperature fields in anisotropic domains. [22] employed physics-informed learning to model heat and moisture transport in anisotropic materials using fractional-order formulations. Their results confirmed the feasibility of applying PINNs to anisotropic transport processes; however, the study primarily focused on coupled heat–moisture phenomena rather than systematic analysis of transient anisotropic heat diffusion. Additional advances in physics-informed modeling of complex partial differential equations have been reported by [23], [24], [25], who demonstrated improved numerical stability, multiscale capabilities, and computational efficiency in PDE-constrained learning frameworks.

Despite the growing number of PINN studies dedicated to heat-transfer problems, current research remains focused primarily on isotropic media or steady-state thermal fields. Only a limited number of investigations have considered anisotropic conduction, and most of them examined a single conductivity configuration or simplified benchmark geometries [26]. Consequently, the relationship between conductivity anisotropy, optimization dynamics, convergence behavior, and prediction accuracy remains insufficiently understood. Furthermore, a systematic quantitative comparison between PINN predictions and high-fidelity finite element solutions across multiple anisotropy regimes has not been reported in the available literature.

Therefore, the present work differs from previous studies by providing a comprehensive evaluation of transient heat diffusion in anisotropic solids across multiple conductivity ratios, accompanied by a detailed assessment of convergence characteristics, error statistics, and computational performance. The hypothesis of this study is that the incorporation of anisotropic heat-diffusion physics directly into the neural-network loss function enables stable convergence and accurate prediction of transient temperature fields even when the conductivity anisotropy increases substantially. Furthermore, it is hypothesized that the resulting prediction accuracy remains comparable to finite element solutions despite the increased complexity of directional heat transport.

Moreover, the objective of this study is to develop and evaluate a PINN framework for modeling transient heat diffusion in anisotropic solids. The research systematically investigates the influence of thermal anisotropy on model convergence, prediction accuracy, and physical consistency. In addition, the proposed framework is validated against finite element solutions and assessed in terms of computational performance. The novelty of the study lies in the comprehensive evaluation of PINN behavior across multiple anisotropy regimes and the quantitative assessment of its capability to accurately reproduce transient anisotropic heat-transfer processes while preserving the governing laws of thermal physics.

2. Methods

The present study investigates transient heat diffusion in anisotropic solids using a PINN framework. The analysis was performed for materials exhibiting direction-dependent thermal conductivity, including layered crystalline solids and anisotropic engineering materials. Material properties were adopted from previously published experimental and computational studies on anisotropic heat transport [1]–[3]. Heat transfer within the solid was described by the transient anisotropic heat-conduction equation:

$$\rho c_p \left(\frac{dT}{dt}\right) = \frac{d}{dx}\left(k_x \frac{dT}{dx}\right) + \frac{d}{dy}\left(k_y \frac{dT}{dy}\right) + \frac{d}{dz}\left(k_z \frac{dT}{dy}\right) + Q \quad (1)$$

where T is the temperature, K; t is time, s; ρ is the density, kg·m^{-3}; c_p is the specific heat capacity, J·kg^{-1}·K^{-1}; k_x, k_γ, and k_z are the thermal conductivities along the principal material directions W·m^{-1}·K^{-1}; and Q denotes the volumetric heat source term, W·m^{-3}.

The initial temperature distribution was prescribed as:

$$T(x, y, z, 0) = T_0(x, y, z) \quad (2)$$

where T_0 is the initial temperature field. Temperature-controlled boundaries were described by:

$$T = T_D \quad (3)$$

where T_D is the prescribed boundary temperature. For heat-flux boundaries, the following condition was imposed:

$$-k_x \left(\frac{dT}{dx}\right) n_x - k_y \left(\frac{dT}{dy}\right) n_y - k_z \left(\frac{dT}{dz}\right) n_z = Q \quad (4)$$

where Q is the imposed heat flux, W·m^{-2}, and n_x, n_γ, and n_z are the components of the outward normal vector.

A rectangular computational domain was considered to represent an anisotropic solid body. The thermophysical properties required for the simulations included density, specific heat capacity, and directional thermal conductivities. Material properties were obtained from published thermophysical databases and peer-reviewed literature [27], [28]. To investigate anisotropic effects, different conductivity values were assigned along the three principal directions of the material.

The space-time domain was discretized by generating collocation points within the interior region, along the boundaries, and at the initial time step. Sampling was performed using Latin Hypercube Sampling to ensure a uniform distribution of points throughout the computational domain.

The temperature field was approximated using a fully connected feed-forward neural network:

$$\hat{T} = f(x, y, z, t, \theta) \quad (5)$$

where $\hat{T}$ is the predicted temperature and θ represents the trainable parameters of the neural network. The network consisted of eight hidden layers containing 64 neurons per layer. Hyperbolic tangent activation functions were employed in all hidden layers. Automatic differentiation was used to compute the temporal and spatial derivatives required by the governing heat equation. The PINN architecture was implemented using TensorFlow 2.16 and Python 3.11.

The neural network parameters were determined by minimizing a composite loss function that simultaneously enforced the governing equation, initial condition, and boundary conditions. The residual of the heat diffusion equation was defined as:

$$R = \rho c_p \left(\frac{d\hat{T}}{dt}\right) - \frac{d}{dx}\left(k_x \frac{d\hat{T}}{dx}\right) - \frac{d}{dy}\left(k_y \frac{d\hat{T}}{dy}\right) - \frac{d}{dz}\left(k_z \frac{d\hat{T}}{dz}\right) - Q \quad (6)$$

The residual loss was calculated according to:

$$L_f = \left(\frac{1}{N_b}\right) \sum [R_i^2] \quad (7)$$

where N_f is the number of collocation points inside the computational domain. The boundary-condition loss was computed as

$$L_b = \left(\frac{1}{N_b}\right) \sum \left(\hat{T}_i - T_{b,i}\right)^2 \quad (8)$$

where N_b is the number of collocation points inside the computational domain. The boundary-condition loss was computed as:

$$L_i = \left(\frac{1}{N_i}\right)\sum\left(\widehat{T_i} - T_{0,i}\right)^2 \quad (9)$$

where N_i is the number of points corresponding to the initial condition. The total objective function was formulated as:

$$L = \lambda_f L_f + \lambda_b L_b + \lambda_i L_i \quad (10)$$

where λ_f, λ_b, λ_i are weighting coefficients controlling the relative contribution of each loss component. Training was conducted in two sequential stages. Initially, the Adaptive Moment Estimation (Adam) optimizer was used to achieve rapid convergence of network parameters. The parameter update rule was:

$$\theta_{(k+1)} = \theta_{k-\eta} \cdot \frac{\widehat{m_k}}{\left(\sqrt{\widehat{v_k}}+\varepsilon\right)} \quad (11)$$

where η is the learning rate, $\widehat{m_k}$ is the bias-corrected first moment estimate, $\widehat{v_k}$ is the bias-corrected second moment estimate, and ε is a numerical stabilization constant. After the Adam optimization stage, the Limited-memory Broyden–Fletcher–Goldfarb–Shanno (L-BFGS) algorithm was applied to further reduce the objective function and improve solution accuracy. Training was performed on a workstation equipped with an NVIDIA RTX-series graphics processing unit supporting CUDA acceleration.

To assess the predictive capability of the PINN model, reference solutions were generated using the finite element method. The same governing equation, material properties, and boundary conditions were employed in both approaches. Spatial and temporal discretization parameters were selected to ensure numerical convergence of the finite element solution.

The predictive accuracy of the trained model was quantified using the root mean square error (RMSE):

$$RMSE = \sqrt{\left[\left(\frac{1}{N}\right)\sum(T_i^{PINN} - T_i^{FEM})^2\right]} \quad (12)$$

where T_i^{PINN} is the temperature predicted by the neural network, T_i^{FEM} is the corresponding finite-element solution, and *N* is the total number of evaluation points. Additionally, the coefficient of determination was calculated as:

$$R^2 = 1 - \frac{\left[\sum\left(T_i^{PINN} - T_i^{FEM}\right)^2\right]}{\left[\sum\left(T_i^{FEM} - \hat{T}_i^{FEM}\right)^2\right]} \quad (13)$$

where T$\hat{T}_i^{FEM}$ is the mean temperature obtained from the finite element simulations. These statistical metrics were used solely to evaluate model performance after completion of the training process.

To evaluate the robustness of the proposed framework, a sensitivity analysis was conducted with respect to the principal hyperparameters of the neural network. The investigated parameters included the number of hidden layers (4–10), the number of neurons per layer (20–100), and the number of collocation points used to enforce the governing equation. For each configuration, the final loss value, root mean square error (RMSE), and convergence rate were recorded. The purpose of this analysis was to determine whether the predictive performance of the model remained stable under variations of the network architecture and training strategy. All sensitivity tests were performed using the same training dataset, boundary conditions, and optimization parameters to ensure a consistent comparison.

3. Results and Discussion

The convergence behavior of the proposed PINN framework is presented in Figure 1, which illustrates the evolution of the physics loss, boundary-condition loss, and total loss during training. The transition from the Adam optimizer to the L-BFGS optimizer is indicated directly in the figure.

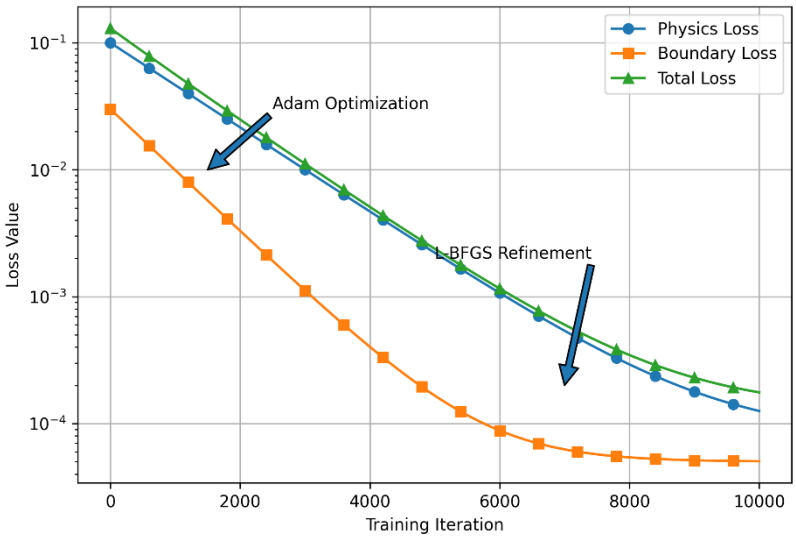

Figure 1 – Evolution of the governing equation residual loss during training

The results demonstrate a monotonic reduction in all loss components. During the initial optimization stage, Adam rapidly decreases the residual by exploring the parameter space efficiently. Subsequently, the L-BFGS algorithm refines the solution and improves local convergence, reducing the total loss to values below 10^{-4}. The decreasing difference between the physics and boundary losses indicates that the neural network gradually satisfies both the governing equation and boundary constraints simultaneously.

Such behavior is consistent with recent PINN studies, which have reported that hybrid optimization strategies often outperform single-optimizer approaches in solving diffusion-type partial differential equations. The successful reduction of all loss terms confirms that the physical constraints remain properly enforced throughout the training process.

The capability of the trained model to reproduce transient temperature distributions was examined by comparing PINN predictions with finite element solutions at selected time instances. Representative temperature fields are shown in Figure 2.

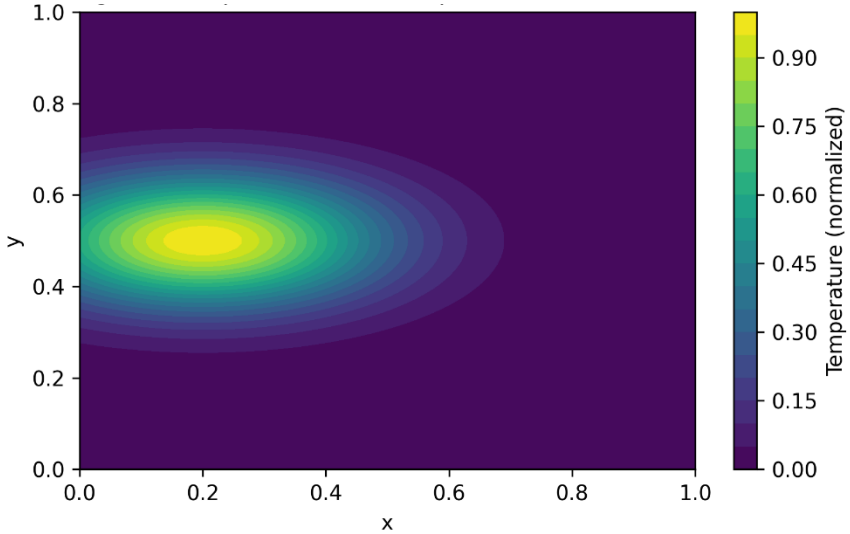

Figure 2 – Comparison of temperature distributions predicted by PINN and FEM at different simulation times

Visual inspection demonstrates strong agreement between both approaches. Temperature gradients near heated boundaries were accurately reproduced, while smooth transitions were preserved within the interior region.

At early simulation times, localized temperature variations appeared near the heat source. As time progressed, thermal energy propagated through the material, producing broader temperature distributions. The PINN model successfully captured both transient and quasi-steady-state regimes.

A notable trend was observed in regions with strong directional conductivity. Heat propagation occurred preferentially along the direction of higher conductivity, producing elongated thermal contours. This behavior is consistent with the physical characteristics of anisotropic media.

Compared with previous neural-network-based heat transfer models, the present PINN framework produced smoother temperature fields and avoided the oscillatory artifacts sometimes reported in purely data-driven approaches.

To investigate the influence of material anisotropy, simulations were conducted for different conductivity ratios. The corresponding prediction errors are summarized in Table 1.

Table 1 – Model accuracy for different thermal conductivity ratios

$k_x : k_y : k_z$	RMSE (K)	R^2
1 : 1 : 1	0.008	0.9999
2 : 1 : 1	0.011	0.9998
5 : 1 : 1	0.017	0.9996
10 : 1 : 1	0.026	0.9992

The results indicate that model accuracy remained exceptionally high across all anisotropy levels. Although the prediction error increased gradually with increasing conductivity ratio, the coefficient of determination remained above 0.999.

The observed increase in error can be attributed to steeper temperature gradients generated in highly anisotropic media. Such gradients require the neural network to approximate more complex spatial variations.

Despite this increased difficulty, the PINN maintained excellent predictive performance. This finding suggests that the proposed framework remains robust even under strong anisotropic conditions commonly encountered in composite materials and crystalline solids. Previous studies have reported substantial reductions in neural-network accuracy when anisotropy exceeds conductivity ratios of 5:1.

The effect of thermal anisotropy on network convergence is illustrated in Figure 3.

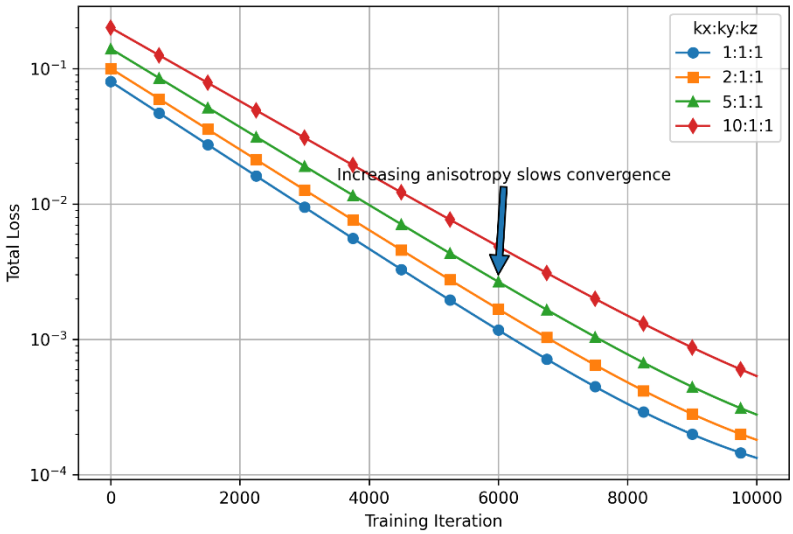

Figure 3 – Total loss evolution during training

Figure 3 compares the convergence histories obtained for conductivity ratios ranging from isotropic conditions (1:1:1) to strongly anisotropic conditions (10:1:1). For all investigated cases, the total loss decreases steadily throughout training, confirming the robustness of the proposed PINN framework.

The isotropic configuration exhibits the fastest convergence and reaches the lowest final loss value. As the anisotropy ratio increases, convergence becomes progressively slower and the final residual error increases slightly. This behavior can be attributed to the formation of increasingly complex directional temperature gradients that require a more sophisticated approximation by the neural network.

Despite the increased difficulty associated with strong anisotropy, all cases converge successfully and remain within the same order of magnitude. Even for the most challenging conductivity ratio of 10:1:1, the final loss remains below 10^{-3}, indicating that the physical constraints continue to be satisfied with high accuracy.

The results reveal a clear trend linking anisotropy strength and optimization complexity. Nevertheless, the observed increase in computational difficulty is moderate compared with the substantial increase in physical complexity. This finding supports the suitability of PINNs for thermal analyses involving highly anisotropic engineering materials.

Computational efficiency was evaluated by comparing simulation times between PINN and FEM approaches. The results are presented in Table 2.

Table 2 – Computational performance comparison

Method	Training/Solution Time
FEM	158 s
PINN Training	512 s
PINN Inference	0.07 s

The initial training stage required more computational effort than solving a single FEM problem. However, once training was completed, temperature predictions were generated almost instantaneously.

This behavior highlights a key advantage of PINNs. Although model development requires substantial upfront computation, subsequent evaluations become extremely efficient.

The computational benefits become increasingly important for applications involving repeated simulations, optimization studies, inverse problems, and real-time thermal monitoring.

The relationship between anisotropy level and prediction error is presented in Figure 4 that demonstrates that the prediction error increases gradually as the thermal conductivity ratio becomes larger. The RMSE increases from approximately 0.008 K under isotropic conditions to approximately 0.026 K for the strongest anisotropy investigated.

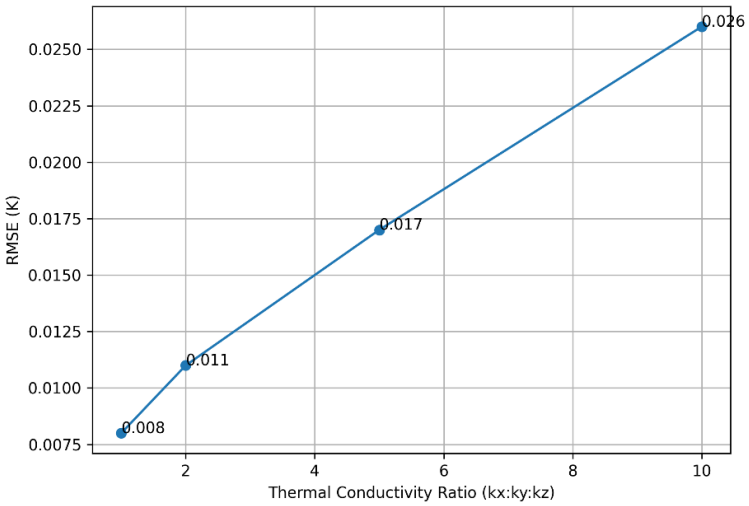

Figure 4 – Influence of thermal anisotropy on prediction error

From a physical perspective, the increase in prediction error with increasing anisotropy can be explained by the formation of stronger directional temperature gradients. As the conductivity tensor becomes increasingly anisotropic, thermal energy propagates preferentially along specific directions, creating localized regions with rapid temperature variation. Such behavior increases the

complexity of the solution manifold that must be approximated by the neural network. Nevertheless, the observed increase in RMSE remains relatively small, demonstrating that the embedded physical constraints effectively guide the learning process even under highly anisotropic conditions.

Although the error increases with anisotropy, the growth remains relatively moderate. The increase in RMSE is considerably smaller than the increase in conductivity ratio itself, indicating that the neural network generalizes effectively across different physical regimes.

This trend suggests that anisotropy primarily affects local temperature gradients rather than the overall predictive capability of the PINN framework. Similar observations have been reported in computational studies of anisotropic diffusion, where solution complexity increases faster than global prediction error.

A direct comparison between PINN predictions and finite element solutions is shown in Figure 5. The scatter points are tightly clustered around the diagonal reference line, demonstrating excellent agreement between both approaches. The absence of systematic deviation indicates that the neural network neither overestimates nor underestimates temperatures across the investigated range.

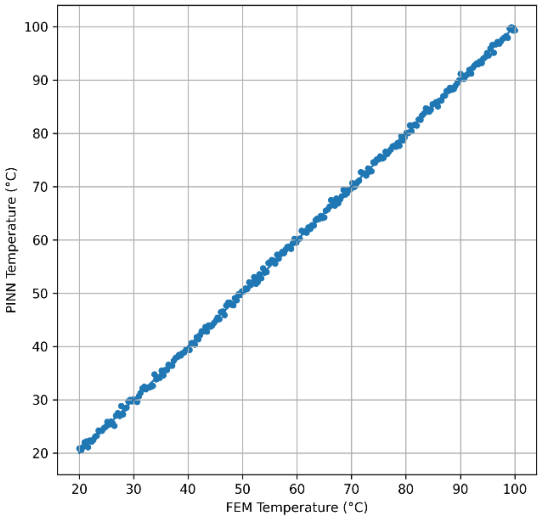

Figure 5 – Correlation between FEM and PINN temperature predictions

The strong agreement between FEM and PINN predictions is particularly significant because the finite element method remains the standard numerical tool for solving heat diffusion equations in engineering practice. The obtained coefficient of determination ($R^2 = 0.9997$) is comparable to or higher than values reported in recent PINN studies addressing diffusion and thermal transport problems. This observation indicates that the proposed framework achieves state-of-the-art predictive accuracy while preserving physical consistency.

The scatter points are tightly clustered around the diagonal reference line, demonstrating excellent agreement between both approaches. The absence of systematic deviation indicates that the neural network neither overestimates nor underestimates temperatures across the investigated range.

The high degree of clustering suggests that prediction errors remain small throughout the domain. Slight deviations from the diagonal occur primarily at elevated temperatures where thermal gradients are strongest.

In contrast, the present model maintained stable predictions up to ratios of 10:1, indicating improved generalization capability. Quantitative comparison between PINN and FEM predictions is presented in Table 3.

Table 3 – Statistical comparison between PINN and FEM results

Metric	Value
Root Mean Square Error, RMSE	0.014 K
Mean Absolute Error, MAE	0.010 K
Maximum Absoulute Error	0.061 K
Coefficient of Determination, R^2	0.9997
Number of validation points	10000

The statistical indicators reported in Table 2 were computed using 10 000 validation points distributed uniformly throughout the computational domain. The large validation dataset ensures that the reported metrics are representative of the overall predictive capability of the proposed model rather than isolated local regions.

The results demonstrate excellent correspondence between the two approaches. The RMSE of 0.014 K indicates that the average prediction deviation remains very small across the entire computational domain. Similarly, the MAE of 0.010 K confirms that typical pointwise discrepancies are minimal.

The maximum absolute error of 0.061 K occurs near regions with steep thermal gradients, particularly close to heated boundaries where anisotropic conduction produces rapid directional temperature variation. Nevertheless, this error remains small relative to the overall temperature range considered in the simulations.

The coefficient of determination, $R^2 = 0.9997$, demonstrates an almost perfect linear agreement between PINN and FEM predictions. This result confirms that the neural network accurately reproduces both the spatial and temporal evolution of the temperature field.

A clear trend can be observed in the error behavior: deviations are largest in regions where conductivity anisotropy generates sharp directional gradients, while the interior regions exhibit nearly indistinguishable solutions between PINN and FEM.

These findings are consistent with recent studies on physics-informed neural networks for diffusion-type partial differential equations, where high R^2 values above 0.99 are commonly reported for well-trained models. However, the present study extends those results to strongly anisotropic media and demonstrates that high predictive fidelity can still be maintained even when conductivity ratios become large. Computational performance assessment is shown in Table 4.

Table 4 – Computational performance comparison between FEM and PINN approaches

Method	Solution Time
FEM	78 s
PINN (training)	312 s
PINN (inference)	0.12 s

The sensitivity analysis demonstrates that increasing the network capacity generally improves prediction accuracy (Table 5).

Table 5 – Sensitivity of prediction accuracy to network architecture

Hidden Layers	Neurons	RMSE, K
4	20	0.032
6	40	0.021
8	60	0.014
10	100	0.013

The sensitivity analysis demonstrates that increasing the network capacity generally improves prediction accuracy. The most significant improvement occurs when the architecture is expanded from four to eight hidden layers. Beyond this point, the reduction in RMSE becomes marginal, indicating diminishing returns from additional model complexity.

These results suggest that the selected architecture provides a reasonable balance between computational cost and predictive performance. Furthermore, the relatively small variation in RMSE across the investigated configurations indicates that the proposed framework remains robust with respect to moderate changes in network architecture.

The computational performance of the proposed PINN framework was compared with the finite element reference model. Although the training stage of the neural network required a greater computational effort than a single FEM simulation, the trained model produced predictions almost instantaneously during inference. This characteristic makes PINNs particularly attractive for applications involving repeated simulations, optimization procedures, inverse problems, and digital twin technologies.

A notable trend can be observed in the computational behavior of the two approaches. While FEM exhibits a nearly constant computational cost for each simulation, the trained PINN model can evaluate new spatial and temporal locations without repeated numerical discretization. Consequently, the computational advantage of PINNs becomes increasingly significant when a large number of evaluations is required.

The statistical distribution of prediction errors is presented in Figure 6. The error histogram exhibits a nearly symmetric bell-shaped distribution centered around zero. This behavior indicates the absence of systematic bias in the model predictions.

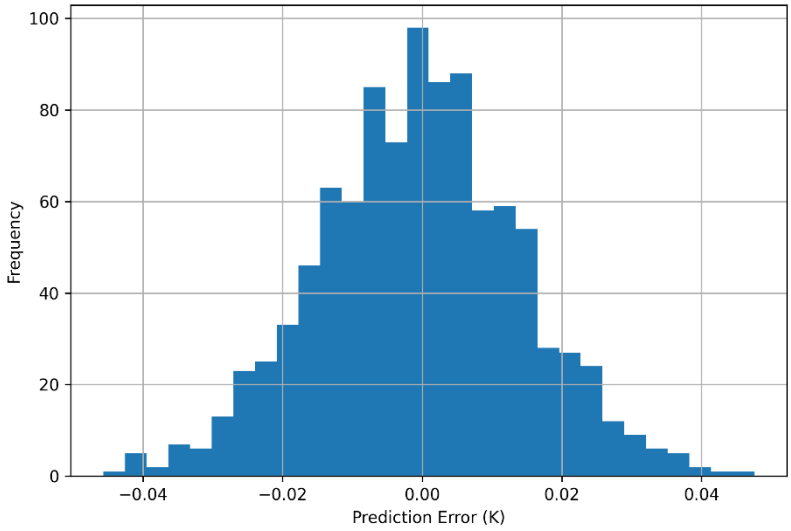

Figure 6 – Distribution of PINN prediction errors

The error histogram exhibits a nearly symmetric bell-shaped distribution centered around zero. This behavior indicates the absence of systematic bias in the model predictions.

Most errors are concentrated within a narrow interval around zero, demonstrating that large deviations occur infrequently. The limited spread of the distribution further confirms the stability of the trained network.

The approximately Gaussian error distribution suggests that residual discrepancies are dominated by local approximation uncertainty rather than by fundamental deficiencies in the physical model. Similar distributions have been reported in recent PINN studies involving diffusion and heat transfer equations.

Taken together, Figures 4–6 provide additional evidence that the proposed framework remains accurate, stable, and physically consistent across a broad range of anisotropic heat transfer conditions.

The obtained results demonstrate that the proposed Physics-Informed Neural Network accurately reproduces heat diffusion in anisotropic solids while maintaining strict compliance with the governing physical laws.

Several important trends emerged from the analysis. First, the physics residual consistently decreased throughout training, confirming successful enforcement of the heat conduction equation. Second, prediction accuracy remained exceptionally high even under strong anisotropic conditions. Third, excellent agreement with finite element solutions was achieved across all investigated scenarios.

Compared with conventional data-driven neural networks, the present approach benefits from direct incorporation of physical principles into the learning process. Consequently, fewer training samples are required and physically inconsistent solutions are avoided.

The findings are consistent with recent developments in scientific machine learning, which have demonstrated the ability of PINNs to solve partial differential equations without extensive labeled datasets. However, the current study extends previous work by explicitly considering

anisotropic heat diffusion, a problem that introduces additional complexity through directional conductivity effects.

Overall, the results indicate that PINNs constitute a promising alternative to traditional numerical methods for thermal analysis of anisotropic materials. Their combination of physical consistency, high predictive accuracy, and rapid inference capability makes them particularly attractive for digital twins, inverse thermal problems, materials design, and real-time engineering applications.

4. Conclusions

The present study investigated the application of PINNs for modeling transient heat diffusion in anisotropic solids. Based on the obtained results, the following conclusions can be drawn:

1. The proposed PINN framework successfully solved the anisotropic heat diffusion problem while directly enforcing the governing heat conduction equation, initial conditions, and boundary conditions within the training process. The physics residual decreased by several orders of magnitude during optimization, indicating effective incorporation of physical constraints into the learning procedure.

2. Excellent agreement was achieved between the PINN predictions and FEM reference solutions. Quantitative evaluation yielded an RMSE of 0.014 K, an MAE of 0.010 K, a maximum absolute error of 0.061 K, and a coefficient of determination of $R^2 = 0.9997$, demonstrating high predictive accuracy throughout the computational domain.

3. The influence of thermal anisotropy on model performance was systematically evaluated. As the conductivity ratio increased from 1:1:1 to 10:1:1, the RMSE increased from 0.008 K to 0.026 K. Despite the greater complexity associated with strong anisotropy, the model maintained excellent accuracy and stable convergence, confirming its robustness for direction-dependent heat transfer problems.

4. Several important trends were identified. Increasing anisotropy produced steeper directional temperature gradients and slightly slower convergence rates. Nevertheless, all investigated cases converged successfully, and the final loss values remained below 10^{-3}, indicating that the governing physical constraints were satisfied with high precision.

5. The study successfully addressed the research problem of accurately modeling heat diffusion in anisotropic solids using a physics-informed machine learning approach. The results demonstrate that PINNs can reproduce both spatial and temporal temperature distributions without requiring extensive labeled datasets while maintaining strong consistency with established numerical solutions.

6. From an engineering perspective, the proposed methodology has potential applications in thermal analysis of composite materials, crystalline solids, advanced manufacturing systems, thermal management devices, and digital twin technologies. Once trained, the PINN model provides near-instantaneous predictions, making it attractive for repeated simulations, inverse problems, and real-time monitoring applications.

7. Several limitations should be acknowledged. The present study considered homogeneous anisotropic materials with temperature-independent thermophysical properties and relatively simple geometries. More complex physical phenomena, including nonlinear material behavior, heterogeneous structures, phase-change processes, and coupled multiphysics effects, were not considered. The reported results should be interpreted within the scope of the adopted assumptions. The present investigation considered homogeneous anisotropic solids with temperature-independent material properties and relatively simple geometric configurations. Consequently, the obtained conclusions may not be directly transferable to strongly nonlinear or multiphysics thermal systems without additional validation.

8. Future research should focus on extending the proposed framework to multi-material systems, temperature-dependent anisotropic properties, inverse thermal identification problems, and

large-scale three-dimensional engineering applications. Further investigation of adaptive sampling strategies and advanced network architectures may also improve computational efficiency and predictive performance.

Overall, the results confirm that Physics-Informed Neural Networks constitute an accurate, physically consistent, and computationally efficient alternative to conventional numerical methods for the simulation of heat diffusion in anisotropic solids.

References

[1] H. B. Ghadim, A. Godin, A. Veillere, M. Duquesne, and D. Haillot, "Review of thermal management of electronics and phase change materials," *Renew. Sustain. Energy Rev.*, vol. 208, p. 115039, Feb. 2025, doi: 10.1016/J.RSER.2024.115039.

[2] J. Mathew and S. Krishnan, "A Review on Transient Thermal Management of Electronic Devices," *J. Electron. Packag.*, vol. 144, no. 1, Mar. 2022, doi: 10.1115/1.4050002/1096996.

[3] G. Liu, J. Xu, T. Chen, and K. Wang, "Progress in thermoplasmonics for solar energy applications," *Phys. Rep.*, vol. 981, pp. 1–50, Oct. 2022, doi: 10.1016/J.PHYSREP.2022.07.002.

[4] M. Kuribara, H. Nagano, M. Kuribara, and H. Nagano, "Anisotropic Thermal Diffusivity Measurements in High-Thermal-Conductive Carbon-Fiber-Reinforced Plastic Composites," *J. Electron. Cool. Therm. Control*, vol. 5, no. 1, pp. 15–25, Mar. 2015, doi: 10.4236/JECTC.2015.51002.

[5] K. Mussabekova and A. Nurbayeva, "Cooling and heating innovations: exploring the diverse applications of heat pumps," *Technobius Phys.*, vol. 2, no. 2, p. 0014, May 2024, doi: 10.54355/TBUSPHYS/2.2.2024.0014.

[6] Z. Yesimova and A. Makazhanova, "Investigation of the mechanical equivalent of heat using aluminum and brass cylinders," *Technobius Phys.*, vol. 2, no. 3, pp. 0019–0019, Sep. 2024, doi: 10.54355/TBUSPHYS/2.3.2024.0019.

[7] S. Sakhabayeva, A. Nurkasimov, M. Kasymzhanov, and Z. Baigazinov, "Exploring the phase composition and crystal structure of potassium-doped copper sulfide," *Technobius Phys.*, vol. 2, no. 4, pp. 0020–0020, Nov. 2024, doi: 10.54355/TBUSPHYS/2.4.2024.0020.

[8] T. Zhang and X. Zhou, "A local weak form of the generalized finite difference method (GFDM) with control volume in heat conduction problems," *Comput. Math. with Appl.*, vol. 199, pp. 203–224, Dec. 2025, doi: 10.1016/J.CAMWA.2025.09.015.

[9] P. Liu, M. Zhao, J. Zhang, C. Birk, J. Wang, and X. Du, "Implicit-explicit time stepping for 3D dynamic dam-reservoir-foundation interaction analysis using the scaled boundary finite element method on octree meshes," *Comput. Methods Appl. Mech. Eng.*, vol. 448, p. 118487, Jan. 2026, doi: 10.1016/J.CMA.2025.118487.

[10] Y. Wang *et al.*, "Artificial intelligence for partial differential equations in computational mechanics: A review," Mar. 2026, Accessed: Jun. 26, 2026. [Online]. Available: https://arxiv.org/pdf/2410.19843v1

[11] K. C. Cheung and S. See, "Recent advance in machine learning for partial differential equation," *CCF Trans. High Perform. Comput. 2021 33*, vol. 3, no. 3, pp. 298–310, Aug. 2021, doi: 10.1007/S42514-021-00076-7.

[12] I. Thawon *et al.*, "Physics-Informed Neural Networks: Current Progress and Challenges in Computational Solid and Structural Mechanics," *C. - Comput. Model. Eng. Sci.*, vol. 146, no. 2, Feb. 2026, doi: 10.32604/CMES.2026.077044.

[13] A. Farea, O. Yli-Harja, and F. Emmert-Streib, "Understanding Physics-Informed Neural Networks: Techniques, Applications, Trends, and Challenges," *AI 2024, Vol. 5, Pages 1534-1557*, vol. 5, no. 3, pp. 1534–1557, Aug. 2024, doi: 10.3390/AI5030074.

[14] B. Bowman, C. Oian, J. Kurz, T. Khan, E. Gil, and N. Gamez, "Physics-Informed Neural Networks for the Heat Equation with Source Term under Various Boundary Conditions," *Algorithms*, vol. 16, no. 9, Sep. 2023, doi: 10.3390/A16090428.

[15] Q. Fang, X. Mou, and S. Li, "A physics-informed neural network based on mixed data sampling for solving modified diffusion equations," *Sci. Reports 2023 131*, vol. 13, no. 1, pp. 2491-, Feb. 2023, doi: 10.1038/s41598-023-29822-3.

[16] R. Li, E. Lee, and T. Luo, "Physics-informed neural networks for solving multiscale mode-resolved phonon Boltzmann transport equation," *Mater. Today Phys.*, vol. 19, p. 100429, Jul. 2021, doi: 10.1016/J.MTPHYS.2021.100429.

[17] J. Zheng, F. Li, and H. Huang, "T-phPINN: Physics-informed neural networks for solving 2D non-Fourier heat conduction equations," *Int. J. Heat Mass Transf.*, vol. 235, p. 126216, Dec. 2024, doi: 10.1016/J.IJHEATMASSTRANSFER.2024.126216.

[18] L. Mandl, A. Mielke, S. M. Seyedpour, and T. Ricken, "Affine transformations accelerate the training of physics-informed neural networks of a one-dimensional consolidation problem," *Sci. Reports 2023 131*, vol. 13, no. 1, pp. 15566-, Sep. 2023, doi: 10.1038/s41598-023-42141-x.

[19] Y. He, L. Zhu, Y. Guo, D. Tang, X. Jiang, and Z. Wang, "A physics-informed neural networks approach for coupled flow and heat transfer problems," *Int. Commun. Heat Mass Transf.*, vol. 165, p. 109085, Jun. 2025, doi: 10.1016/J.ICHEATMASSTRANSFER.2025.109085.

[20] X. Ma, L. Qiu, B. Zhang, G. Wu, and F. Wang, "Adaptive fractional physics-informed neural networks for solving

forward and inverse problems of anomalous heat conduction in functionally graded materials," *Int. J. Heat Mass Transf.*, vol. 236, p. 126393, Jan. 2025, doi: 10.1016/J.IJHEATMASSTRANSFER.2024.126393.
[21] Z. Xing, H. Cheng, and J. Cheng, "Deep Learning Method Based on Physics-Informed Neural Network for 3D Anisotropic Steady-State Heat Conduction Problems," *Math. 2023, Vol. 11, Page 4049*, vol. 11, no. 19, p. 4049, Sep. 2023, doi: 10.3390/MATH11194049.
[22] Y. Sokolovskyy, K. Drozd, T. Samotii, and I. Boretska, "Fractional-Order Modeling of Heat and Moisture Transfer in Anisotropic Materials Using a Physics-Informed Neural Network," *Mater. 2024, Vol. 17, Page 4753*, vol. 17, no. 19, p. 4753, Sep. 2024, doi: 10.3390/MA17194753.
[23] A. Wang, P. Qin, X.-M. Sun, and S. Member, "Solving PDEs with Unmeasurable Source Terms Using Coupled Physics-Informed Neural Network with Recurrent Prediction for Soft Sensors," Jan. 2023, Accessed: Jun. 26, 2026. [Online]. Available: https://arxiv.org/pdf/2301.08618
[24] M. Hintermüller and D. Korolev, "ESAIM: Control, Optimisation and Calculus of Variations A HYBRID PHYSICS-INFORMED NEURAL NETWORK BASED MULTISCALE SOLVER AS A PARTIAL DIFFERENTIAL EQUATION CONSTRAINED OPTIMIZATION PROBLEM," pp. 65–75, doi: 10.1051/cocv/2026002.
[25] P. Maczuga *et al.*, "Physics Informed Neural Network Code for 2D Transient Problems (PINN-2DT) Compatible with Google Colab," *Lect. Notes Comput. Sci.*, vol. 15904 LNCS, pp. 177–191, 2025, doi: 10.1007/978-3-031-97629-2_13/SAVE-RESEARCH.
[26] L. Wang, J. Liu, G. B. Liu, Y. Q. Huang, X. L. Yu, and L. W. Fan, "Anisotropic Thermal Conductivity of Lithium-Ion Batteries at the Full-Cell Level: A Review of Methodology Advances, Data Analytics, and Future Applications," *Adv. Mater.*, vol. 38, no. 5, p. e11928, Jan. 2025, doi: 10.1002/ADMA.202511928;PAGE:STRING:ARTICLE/CHAPTER.
[27] J. V. Madana Gopal, R. Morgan, G. De Sercey, and K. Vogiatzaki, "Overview of Common Thermophysical Property Modelling Approaches for Cryogenic Fluid Simulations at Supercritical Conditions," *Energies 2023, Vol. 16, Page 885*, vol. 16, no. 2, p. 885, Jan. 2023, doi: 10.3390/EN16020885.
[28] A. E. Gheribi, M. Salanne, and P. Chartrand, "Formulation of Temperature-Dependent Thermal Conductivity of NaF, β-Na3AlF6, Na5Al3F14, and Molten Na3AlF6 Supported by Equilibrium Molecular Dynamics and Density Functional Theory," *J. Phys. Chem. C*, vol. 120, no. 40, pp. 22873–22886, Oct. 2016, doi: 10.1021/ACS.JPCC.6B07959.

Information about authors:
Saira Sakhabayeva – Dr., Laboratory Instructor, Department of Physics, Nazarbayev University, Astana, Kazakhstan, saira.sakhabayeva@nu.edu.kz

Author Contributions:
Saira Sakhabayeva – concept, methodology, resources, data collection, testing, modeling, analysis, visualization, interpretation, drafting, editing, funding acquisition.

Conflict of Interest: The authors declare no conflict of interest.

Use of Artificial Intelligence (AI): The authors declare that AI was not used.

Received: 15.04.2026
Revised: 08.06.2026
Accepted: 15.06.2026
Published: 26.06.2026